Mol Neurobiol (2012) 45:536–549
DOI 10.1007/s12035-012-8275-8

3′poly-G-Tailed ODNs Inhibit F-spondin to Induce Cell Death and Neurite Retraction in Rat Embryonic Neurons

Yung-Chih Cheng · Tai-An Chen · Chih-Yuan Chen · Chi-Ming Liang · Shu-Mei Liang

Received: 26 February 2012 / Accepted: 1 May 2012 / Published online: 17 May 2012
© Springer Science+Business Media, LLC 2012

Abstract The effects and mechanism of action of oligodeoxyribonucleotides containing CpG motif (CpG-ODNs) on neuron cells are largely unexamined. Here, we found that CpG-A ODNs but not other types of CpG-ODNs induced neurite retraction and cell apoptosis of rat embryonic neurons in a TLR9-independent manner. These effects of CpG-A ODNs were primarily due to the poly-guanosine at the 3′ terminus (3′G-ODNs). Pull-down analysis showed that 3′G-ODNs associated with transcription factor Y-BOX1 (YB-1) to facilitate the translocation of YB-1 into the nucleus via the nuclear localizing sequence of YB-1. YB-1 then interacted with the promoter of F-spondin directly at −45 and −1,375 sites as demonstrated by chromatin immunoprecipitation (ChIP) analysis. Binding of YB-1 to F-spondin promoter resulted in downregulation of F-spondin expression. Overexpression of F-spondin rescued the cell death and neurite retraction induced by 3′G-ODNs in embryonic neuron cells. Taken together, these findings suggest that 3′G-ODNs enhance nucleus YB-1 to inhibit F-spondin leading to cell death and neurite retraction of embryonic neuron cells

Keywords Neuron · F-spondin · YB-1 · 3′G-ODNs

Abbreviation

siRNA	Small interference RNA
TSR	Thrombospondin type 1 repeat
PNS	Peripheral nervous system
PBMC	Peripheral blood mononuclear cell
HLA	Human leukocyte antigen

Introduction

DNA fraction isolated from *Mycobacterium bovis* bacillus Calmette–Guerin activates both human and mouse non-B, non-T cells to produce type I interferons (IFNs) [1]. Such immunostimulation can also be generated by unmethylated single-stranded (ss) oligodeoxyribonucleotides (ODNs) containing CpG dinucleotides with certain flanking sequences (CpG motifs) [2, 3], which have been identified as a ligand for TLR9 [4]. There are three known classes of CpG ODNs: A-class (CpG-A ODNs), B-class (CpG-B ODNs), and C-class CpG ODNs, all of which possess unmethylated CpG dinucleotides. CpG-A ODNs are effective in activating NK cells and stimulating plasmacytoid dendritic cells (pDCs) and macrophages to produce high levels of interferon α (IFN-α) [5, 6]. The activity of CpG-A ODNs to stimulate plasmacytoid dendritic cells (pDCs) is due to their phophodiester CpG-containing palindromic motifs and a poly-G tail at the 3′-end (3′G-ODNs) which is important for self-assembly of CpG-A ODNs into higher-order tertiary structures through G-tetrad formation [7].

DNA and RNA oligomers that contain consecutive guanine (G) nucleotides have the ability to form stable inter- and intramolecular four-stranded secondary structures, referred to as G-quartets [8, 9]. Moreover, G-quartets have been proposed to be involved in the regulation of gene expression and enhancement

Electronic supplementary material The online version of this article (doi:10.1007/s12035-012-8275-8) contains supplementary material, which is available to authorized users.

Y.-C. Cheng
Institute of Biochemical Sciences, National Taiwan University, Taipei, Taiwan

Y.-C. Cheng · T.-A. Chen · C.-Y. Chen · S.-M. Liang (✉)
Agricultural Biotechnology Research Center, Academia Sinica, 128 Academia Road, Section 2, Nangang, Taipei 115, Taiwan
e-mail: smyang@gate.sinica.edu.tw

C.-M. Liang
Genomics Research Center, Academia Sinica, Taipei, Taiwan

of cancer cell apoptosis [10]. Whether CpG-A ODNs or 3′G-ODNs can regulate gene expression and apoptosis of neuronal cells, however, is poorly understood.

F-spondin, a member of the TSR superfamily, is a secreted adhesion molecule isolated from embryonic floor plate of the developing vertebrate central nervous system [11–13]. Because F-spondin mRNA and protein expression is highly unregulated after axotomy of the adult sciatic nerve, it has been suggested that F-spondin may participate in axonal regeneration in the PNS [11, 14]. Nevertheless, the fundamental mechanisms of F-spondin-mediated neuron regeneration or neuron survival are not clearly understood. We previously found that F-spondin was up-regulated in peripheral blood mononuclear cell (PBMC) by CpG-B ODN stimulation [15]. Because CpG-B ODN has capability to induce anti-apoptotic effect in PBMC, it implicates that F-spondin may involve in anti-apoptotic process. Besides, it has recently been reported that F-spondin plays an important role in promoting cell survival in chicken ciliary ganglion and murine neuroblastoma cells [16, 17]. These studies indicate that F-spondin is essential for neuron development and neuron cell survival.

In this study, we found that CpG-A ODNs induced cell aggregation and neurite shrink in TLR-9-expressing embryonic neuron cells. These effects of CpG-A ODNs were mainly mediated by the 3′G-ODNs rather than TLR-9 activation. 3′G-ODNs bound to Y-BOX1 (YB-1) and promoted YB-1 translocation into nucleus. Accumulation of YB-1 in nucleus repressed F-spondin gene expression that in turn induced the cell death and neurite retraction of rat embryonic neuron cells.

Materials and Methods

Animals

Female pregnant Sprague–Dawley rats (Biolasco Co., Taipei) were housed in individual cages. The animals were maintained on a 12-h light/dark cycle with food and water. All animal care and experimental procedures in the animals were performed under protocols approved by the Academia Sinica Institutional Animal Care and Utilization committee.

Reagents

TLR9 ligand, CpG-A ODNs (ODN 1585 and ODN 2216), CpG-B ODNs (ODN1668 and ODN2006), and their controls were purchased from InvivoGen (San Diego, CA). psiGL3 vector (silence control vector) and psi-mTLR9 (mTLR9 silenced plasmid) were also purchased from InvivoGen (San Diego, CA). 3′G-ODNs, 5′G-ODNs, poly-G, FAM-labeled 3′G-ODNs, biotinylated 3′G-ODNs, and biotinylated 5′G-ODNs were synthesized by Genedragon Co. (Taipei, Taiwan). Rabbit polyclonal anti-mTLR9 was purchased from Imgenex (Los Angeles, CA). Rabbit polyclonal anti-F-spondin was purchased from Abcam Biotechnology (Cambridge, UK). The anti-YB-1 and anti-Lamin A/C antibodies were purchased from Epitomics (Burlingame, CA). The anti-hnRNPH1, anti-EF1A1, and anti-ßIII tubulin antibodies were purchased from Genetex Co. (Hsinchu, Taiwan). The anti-actin antibody was purchase from Millipore (Chemicon, CA).

Cell Culture

The human neuroblastoma cell line SH-SY5Y was a gift from Dr. Yu-May Lee (Academia Sinica, Taipei, Taiwan). SH-SY5Y cells were cultured in a 1:1 mixture of Dulbecco's modified Eagle's medium and F12 medium (Gibco, Life Technologies, Taipei) supplemented with 10 % heat-inactivated fetal bovine serum, 100 U/ml penicillin–streptomycin–neomycin antibiotic mixtures, and 200 mM L-glutamine. Cells were cultured in a humidified atmosphere under 5 % CO_2 at 37 °C. In all experiments, the media were changed every 3 days for all experiments.

Isolation and Culture of Primary Rat Embryonic Neuronal Cells

Primary rat neuronal cultures were prepared from embryonic day 18 Sprague–Dawley rat cortices and hippocampus. Briefly, cortices and hippocampus were digested with papain (Sigma-Aldrich, St. Louis, MO) for 30 min at 37 °C. Then, using inactive horse serum to stop digestion, cortices and hippocampus were pipetted about 50 times without bubble formation. The cell suspension was then passed successively through 100-, 70-, and 40-μm mesh and carefully applied to the top of a prepared OptiPrep density gradient [18]. The cell suspension should float on top of the gradient. The gradient was centrifuged at 800×*g* (1,900 r.p.m. in a swinging bucket centrifuge) for 15 min at 22 °C. After centrifugation, the desired cell fractions were mixed and diluted with 5 ml embryonic neuron growth medium (neurobasal media supplemented with 2 % B27, 500 mM *L*-glutamine, 10 mg/ml Gentamicin; Gibco, Life Technologies, Taipei). The cell suspension was subsequently centrifuged at 1,100×*g* for 5 min, and cell pellets were then gently re-suspended in embryonic neuron growth medium. Thereafter, cells were counted and dispensed into poly-D-lysine-coated plates and incubated at 37 °C with 5 % CO_2. After 24 h of plating, the media were completely replaced, while on subsequent days, only half of the culture volume was replaced. Neuron cells were routinely used at day 3 after plating.

Transfection of Embryonic Neuron Cells

Embryonic neuron cells were electroporated with pmax-EGFP vector, pBiotin-F-spondin, or pEGFP-F-spondin plasmids by using a nucleofector device (Amaxa, Germany)

according to the manufacturer's instructions (Rat Neuron Nucleofector Kit, program G-13). After transfection, the embryonic neuron cells were plated on poly-D-lysine-coated plates and incubated at 37 °C with 5 % CO_2. The transfected neuron cells were used after 48 to 72 h for further experiments.

Neurite Outgrowth Analysis

For quantitative analysis of neurite outgrowth, neuron cells were electroporated as described above. After 24 h of treatment with 3′G-ODNs, cells were fixed in 4 % paraformaldehyde and washed with PBS. Neurite outgrowth was quantified by imaging neurons using a Zeiss Axlovert 200 M microscope. Digital images were acquired using the Axiovision system and neurites were quantified using the *Image J* software. For each graph, data on neurite length were generated from at least two independent sets of neurons (for each condition) and more than 50 cells were counted for each condition of each experiment.

Cell Death and Viability Assay

Viability of the embryonic neuron cells was determined by a colorimetric method using the CellTiter 96 One Solution Proliferation Assay (Promega, WI). This assay contains a tetraxolium compound (3-(4,5-dimethylthiazol-2-yl)-5-(3-carboxymethoxy phenyl)-2-(4-sulfophenyl)-2H-tetrazolium, inner salt (MTS)) and an electron-coupling reagent, phenazine methosulfate. The tetrazolium compound is converted to a soluble formazan product by cells. Embryonic neuron cells were plated in a 96-well plate at a cell density of 10^5 cells/cm^2. The reagent was added directly into 96-culture wells performed assay, followed by incubation for 4 h. Then, the absorbance at 490 nm was recorded using a 96-well plate reader. Cell death was determined by propidium iodide (PI) staining. Finally, cells were counted under a fluorescence microscope.

Caspase Enzymatic Activity Assay

To assay for caspase 3/7 activity, embryonic neuron cells were plated in a 96-well white plate at a cell density of 10^5 cells/cm^2. After stimulation with 3′G-ODNs for 72 h at the indicated concentration in independent wells, 100 μl Caspase-Glo 3/7 reagents (Promega, WI) were added to the wells. Then, the 96-well white plate was incubated at room temperature for 3 h and the luminescence determined by using a Wallac 1420 Victor3 micro-plate reader (Perkin-Elmer, CT). Mean values and standard deviations were calculated based on the results from three individual samples of each treatment.

Pull-Down Assay

For the pull-down experiments, 100 μl streptavidin-coupled magnetic beads (Dynabeads M-280 Streptavidin, Invitrogen, Life Technologies, Taipei) were coated with 200 pmols of biotinylated 3′G-ODNs by incubation in 0.8 ml ×1 B & W buffer (100 mM Tris–HCl, pH 7.5, 1 mM EDTA, and 2 M NaCl) for 30 min at room temperature. As a control, 100 μl of Magnetic Dynabeads M-280 streptavidin were coated with 200 pmols of biotinylated 5′G-ODNs. Rat embryonic brain tissue protein was extracted by using the T-PER tissue protein extraction buffer (Thermo Scientific, MA). Protein concentrations were determined by using a Bio-Rad protein assay solution (Bio-Rad, CA). Then, brain tissue lysates were incubated with 3′G-ODNs bound to magnetic beads in 1 ml 1x B & W buffer for 24 h at 4 °C. After washing the beads seven times in PBS, bound protein was removed from the beads by heating in 5x SDS loading sample buffer, the eluted sample was then analyzed by 4–20 % gradient sodium dodecyl sulfate polyacrylamide gel electrophoresis (SDS-PAGE) and detected by staining with Coomassie Blue. Bands were analyzed by tryptic digestion and mass spectrometry. For detection of 3′G-ODN association with YB-1, complexes were separated by SDS-PAGE, subjected to immunoblotting using anti-YB-1 antibody, and visualized by enhanced chemiluminescence (ECL; Pierce, IL) using Hyperfilm (GE Healthcare, NJ).

RNA Isolation and Real-Time Quantitative PCR

Total RNA was extracted from embryonic neuron cells using Trizol reagent (Invitrogen, Life Technologies, Taipei) according to the manufacturer's protocol. One microgram of total RNA was reverse-transcribed using SuperScript III Reverse Transcriptase (Invitrogen, Life Technologies, Taipei). The sequences of forward and reverse oligonucleotide primers were designed using Primer Design software. The primers used are: forward 5′-ACT TCA GAG GTT TCA GGT TAA T-3′ and reverse 5′-CCT TCA GAA TCA CAC AGC C-3′ for F-spondin; forward 5′-TGG AAT CCT GTG GCA TCC ATG AAA C-3′ and reverse 5′-TAA AAC GCA GCT CAG TAA CAG TCC G-3′ for β-actin. Real-time quantitative PCR was performed using Roche Light-Cycler (Roche Diagnostics, IN) and quantified using SYBR Green. Expression levels of F-spondin mRNA were subsequently normalized to the level of β-actin, a housekeeping gene. Statistical analysis was carried out by one-way analysis of variance. Differences were considered significant when $P<0.05$.

Western Immunoblotting

For western blot analysis, cells were harvested in the presence of a protease inhibitor cocktail tablet (Roche Diagnostics, IN)

using mammalian protein extraction buffer (GE Healthcare, NJ). Protein concentrations were determined by using a Bio-Rad protein assay solution (Bio-Rad, CA). Equivalent amounts of protein were loaded and separated by SDS-PAGE and subsequently transferred to a nitrocellulose membrane. After washing in TBS containing Tween-20, blots were blocked in 5 % milk for 1 h at room temperature and incubated with antibodies (described above), followed by incubation with horseradish peroxidase-conjugated secondary antibody for 1 h at room temperature and visualization by ECL. Band intensities were normalized to either actin or lamin A/C for comparison.

Plasmid Constructs and Transient Transfection

The full-length cDNA for the *YB-1* gene was purchased from OriGene (Rockville, MD), and the YB-1 expression construct was generated using the Gateway GFP fusion destination vector pDEST47 (C-terminal GFP fusion, Invitrogen, Life Technologies, Taipei). The full-length cDNA clone for the *F-spondin* gene was purchased from Open Biosystems (Thermo Scientific, IL), and the F-spondin expression construct was generated using pDEST47 or the Gateway vector pcDNA6/BioEase-DEST (N-terminal Biotin fusion, Invitrogen, Life Technologies, Taipei). The plasmid YB-1-dNLS was generated by mutational PCR and the KOD ligation system using the following primer sequences: forward, 5′-CCA CAG TAT TCC AAC CCT C-3′; reverse, 5′-GGC CTG GCC TTC GGG AG-3′. For transient transfection, cells were seeded at a density of 5×10^6 cells/25-cm^2 6-well plate for 24 h. Transfection was performed using the Fugene HD reagent (Roche Diagnostics, IN) according to the manufacturer's protocol. Cells were observed by fluorescence microscopy 48 h after transfection.

Chromatin Immunoprecipitation

Chromatin immunoprecipitation assays were done using the chromatin immunoprecipitation (ChIP)-Mag kit (Millipore,). In brief, embryonic neuron cells were isolated and plated on 10-cm plates in neuron growth medium. After 3 days in vitro, cells were fixed for 10 min with 1 % formaldehyde. After quenching the reaction with glycine for 5 min, cells were lysed with cell lysis buffer (20 mM Tris–HCl, pH 8.0, 85 mM KCl, 0.5 % NP-40). The nuclei were isolated and chromatin was sonicated in shearing buffer using TOMY Ultrasonic Disruptor UD-201 with ten pulses of 15 s each (output=5) and 1-min rest periods on ice between each pulse, resulting in chromatin fragments between 200 bp and 1 kb DNA. Immunoprecipitation was then done using an antibody to YB-1. Chromatin was incubated with 10 μg anti-YB-1 polyclonal antibody overnight at 4 °C. Protein G magnetic beads was subsequently incubated with the chromatin and antibody for 4 h at 4 °C. The immunoprecipitated complex was then washed by ChIP wash buffer and eluted from the magnetic beads by ChIP elution buffer following manufacturer's protocol. The immmunoprecipitated complex was subsequently incubated with 10 μg RNase A for 30 min at 37 °C to reverse cross-links and to remove RNA. The proteins were then removed by proteinase K treatment, and the DNA was purified using the DNA purification mini-columns provided with the kit. The eluted DNA was amplified by PCR with predicted ATTGG sites in the promoter of F-spondin: (−45) forward 5′-CACTATGGCCTTGGGAAGAGCAAT-3′ and reverse 5′-ACTGTATCGACTCGCCTTCATGTT-3′; (−1,137) forward 5′-ACATG GATCTGAGCCTCACCTCAA-3′ and reverse 5′-GCCACTATTAACTGGACGCC TTCT-3′; (−1,847) forward 5′-AGCCATGGAACATTACCTCAGCA-3′ and reverse 5′-GGCATGAAGTAGGCAGGAATGCAA-3′; (−2,045) forward 5′-TGAGTGACAG CCAAGCTGGTTTAG-3′ and reverse 5′-AAAACAGGCATCCCCAACACCA-3′; (−3,075) forward 5′-TTCTTTGGGGAGGCAGTTTTGCAC-3′ and reverse 5′-AAGG CTCTGCTTGATCTGCTTCTC-3′. GAPDH control primers: forward 5′-TACTA GCGGTTTTACGGGCG-3′ and reverse 5′-TCGAACAGGAGGAGCAGAGAGCG A-3′. The PCR program was set with an initial melting step at 94 °C for 5 min, followed by 35 cycles of 94 °C for 30 s, 56 °C for 30 s, and 72 °C for 1 min. The F-spondin primers and control primers produced products of around 150 bp.

Results

CpG-A ODNs Decrease Neurite Length of Embryonic Neuron Cells TLR9 Independently

In order to investigate the biological function of CpG-ODN in neuron cells, we first examine TLR9 expression in embryonic neuron cells. We showed that embryonic hippocampal neurons expressed TLR9 protein by western blotting (Fig. 1a) and confirmed by immunofluorescence staining (Fig. 1 in the Electronic Supplementary Material (ESM)). To investigate whether TLR9 activation induces any biological activity on neuron cells, we treated embryonic neuron cells with two TLR9 ligands, ODN 2006 and ODN 2216, and then observed changes in morphology of embryonic neuron cells. We found that treatment with ODN 2006, a CpG-B ODN, did not change the morphology of embryonic neuron cells; whereas, CpG-A ODN, ODN 2216, induced aggregation of embryonic neuron cells (Fig. 1b).

Because the function of neuron cells depends on neurite extension, we examined the neurite length of embryonic neuron cells after CpG-A ODNs treatment by microscopy. We found that ODN 2216 treatment led to a decrease in neurite length as compared with ODN 2006 treatment (Fig. 1c, d). To further address whether the effect induced

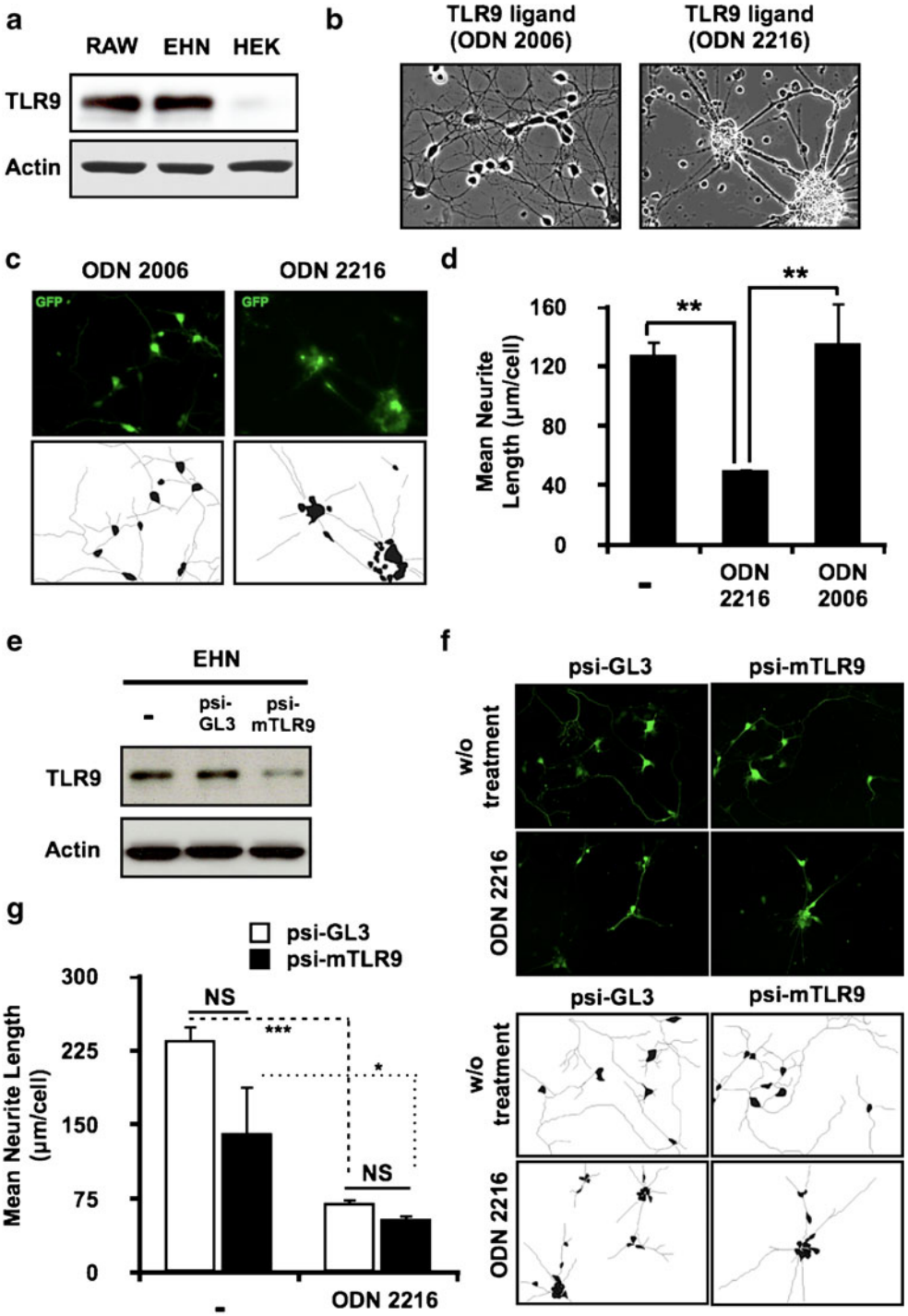

Fig. 1 CpG-A ODNs induced cell aggregation and neurite retraction of embryonic neuron cells TLR9-independently. **a** Embryonic hippocampal neurons (*EHN*) were isolated and purified from E18 SD rat embryo. TLR9 protein expression in RAW264.7 cells (*RAW*), EHN, and human embryonic kidney 293 cells (*HEK*) was analyzed by western blotting. Actin was used as a loading control. **b** After culture of rat embryonic neuron cells for 2 days in vitro, 1 μM CpG-B ODN (*ODN 2006*) or CpG-A ODN (*ODN 2216*) was added directly into the culture medium. After 16 h, the morphology of embryonic neuron cells was observed by microscopy. **c** Embryonic neuron cells were transiently transfected with green fluorescent protein (*GFP*) plasmid and stimulated with 1 μM of TLR9 ligands, ODN 2006, or ODN 2216, 72 h thereafter. The morphology and neurite length of embryonic neuron cells were observed by microscopy and traced by Image J software. **d** The neurite length traced was also quantified by Image J software. Data represent the mean±SD; $^{**}P<0.01$. **e** Embryonic hippocampal neuron cells were transiently transfected with GFP-fused TLR9 siRNA plasmid or psi-GL3 empty vector as indicated. The knock-down of TLR9 was confirmed by western blotting. Actin was used as a loading control. **f** Cells treated as described in (**e**) were stimulated with 1 μM of ODN 2216 72 h thereafter, and the cell morphology and neurite length were observed and traced as described above. The quantification of neurite length is shown in (**g**). Data represent the mean±SD; $^{***}P<0.001$; $^{*}P<0.05$ *NS* not significant

by CpG-A ODNs in embryonic neuron cells is mediated through the TLR9 signaling pathway, embryonic neuron cells were transiently transfected with a TLR9 silencing RNA (psi-mTLR9). Even though psi-mTLR9 reduced TLR9 level considerably (Fig. 1e), ODN2216 treatment still caused aggregation of TLR9-silenced embryonic neuron cells, and the neurite length was not restored in TLR9-silenced embryonic neuron cells either (Fig. 1f, g). Interestingly, the TLR9 control ligand GpC-A ODN (ODN 2216 control) induced neuronal aggregation as CpG-ODN (ODN 2216) (Table 1). Besides, other CpG-A ODNs (ODN 1585) and its control (ODN 1585 control) also induced neuronal aggregation in rat embryonic neurons. However, this effect was absent in rat embryonic neurons treated with CpG-B ODNs (ODN 1668) (Fig. 2 in the ESM). Taken together, these results suggest that neuron morphological

Table 1 Oligodeoxynucleotides investigated

Name	Sequence 5′ to 3′	Class	Neuron aggregation
ODN 1585	GGGGT CAACG TTGAG GGGGG	CpG-A ODN	+
ODN 2216	GGGGG ACGAT CGTCG GGGGG	CpG-A ODN	+
ODN 1668	TCCAT GACGT TCCTG ACGTT	CpG-B ODN	−
ODN 2006	TCGTC GTTTT GTCGT TTTGT CGTT	CpG-B ODN	−
ODN 1585 control	GGGGT CAAGC TTGAG GGGGG	CpG-A ODN control	+
ODN 2216 control	GGGGG AGCAT GCTGG GGGGG	CpG-A ODN control	+
3′G-ODN	ACGAT CGTCG GGGGG	ODN2216 without 5′poly-G	+
5′G-ODN	GGGGG ACGAT CGTC	ODN2216 without 3′poly-G	−
Poly-G	GGGGG GGGGG G	Poly-G	+

change and neurite retraction induced by CpG-A ODNs is not mediated through the effects of CpG-A ODNs on TLR9-dependent signaling pathway.

3′G-ODNs Induce Neuron Cell Aggregation and Neurite Retraction

DNA oligomers that contain consecutive G nucleotides have the ability to form G-quadruplex structures and enhance cell apoptosis [8, 9] To investigate whether the effect induced by CpG-A ODNs on embryonic neuron cells is mediated by its poly-G motifs, we synthesized a 3′G-ODN and a 5′G-ODN (see Table 1) to stimulate embryonic neuron cells and observed the cellular morphology 16 to 24 h after stimulation. We found that the morphology of embryonic neuron cells was changed after 3′G-ODNs treatment, but remained unchanged after 5′G-ODNs treatment (Fig. 2a, top panels). To confirm our finding, the embryonic neuron cells were also transiently transfected with pMaxGFP plasmid before stimulation with 3′G-ODNs in order to trace neurites easily in each neuron. After 24 h of stimulation with 3′G-ODNs, the embryonic neuron cells progressively aggregated and the cellular morphology changed to a spherical structure (Fig. 2a, middle panels). We further found that the neurite spreading became sparse after 3′G-ODNs treatment. Therefore, we calculated the neurite length in each embryonic neuron cell by tracing GFP expression. We observed that neurites of embryonic neuron cells stimulated with 3′G-ODN were shorter than those of embryonic neuron cells that did not receive treatment or were treated with 5′G-ODNs (Fig. 2a, bottom panels). Collectively, the data indicate that the 3′ poly-G of CpG-A ODNs plays a critical role in inducing neuronal aggregation and neurite retraction in embryonic neuron cells.

3′G-ODNs Induce Neuron Cell Apoptosis Through Caspase 3/7 Pathways

It is known that cytoplasmic mutant huntingtin and atypical truncated tau induce neurite regression and cell death in neuron cells [19, 20]. We then examined the cell viability in embryonic neuron cells after 3′G-ODNs treatment. As shown in Fig. 2b, treatment with 3′G-ODNs at the indicated concentration for 48 h inhibited cell viability in embryonic neuron cell. However, the cell viability did not decrease in the 5′G-ODNs-treated group (Fig. 2b). Next, we also confirmed the ability of 3′G-ODNs to induce cell death by PI staining. We found that the number of PI positive cells in embryonic neurons treated with 3′G-ODNs at 2 μM was higher than that in embryonic neuron cells treated with the same concentrations of 5′G-ODNs (Fig. 2c). To examine whether the cell death induced by 3′G-ODNs in embryonic neuron cells occurs through an apoptotic pathway, we further assayed caspase 3/7 activities in embryonic neuron cells after 3′G-ODNs or 5′G-ODNs treatment. The caspase 3/7 activities in 3′G-ODNs-treated embryonic neuron cells were higher than those treated with 5′G-ODNs after 48 h (Fig. 2d). Together, these results indicate that 3′G-ODNs not only induced embryonic neuron cell aggregation and inhibited neurite extension but also increased caspase 3/7 activities and induced apoptotic cell death in embryonic neuron cells.

Association of 3′G-ODNs with YB-1 Protein in the Cytoplasm Enhances Nuclear Translocation of YB-1

We first examined whether embryonic neuron cells take up the 3′G-ODNs, and we found that FAM-labeled 3′G-ODNs mainly localized in the cytoplasm of embryonic neuron cells (Fig. 3 in the ESM). To investigate whether other proteins in the cytoplasm of neuron cells associate with 3′G-ODNs

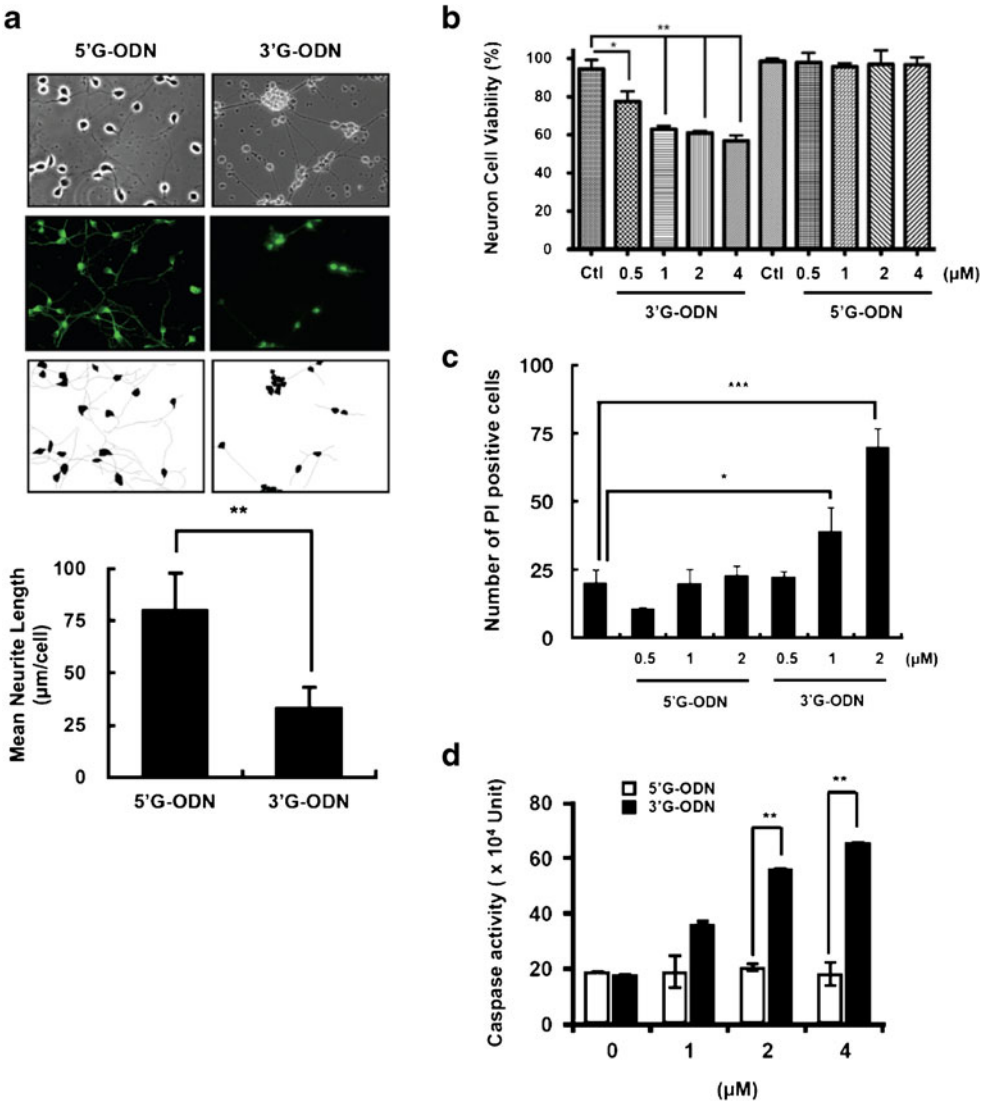

Fig. 2 3′G-ODN treatment induces cytotoxicity and neurite retraction in rat embryonic neuron cells. **a** Representative micrographs of embryonic neuron cells treated with 1 μM of 5′G-ODN or 3′G-ODN at 37 °C for 16 h. Cellular morphology was observed by fluorescence microscopy. Cells were fixed and immunostained with anti-βIII-tubulin (*green*) antibodies. The effect of 3′G-ODN on neurite length was also quantified. **b** Embryonic neuron cells were cultured for 48 h in neurobasal medium in the presence of 5′G-ODN or 3′G-ODN as indicated. MTS assay was used to determine cell viability. **c** Percentage of damaged embryonic neuron cells after 48-h incubation with 5′G-ODN or 3′G-ODN as indicated. **d** The caspase 3/7 activities in embryonic neuron cells treated with 5′G-ODN or 3′G-ODN as indicated for 48 h were estimated. Data represent the mean±SD; $N=3$; *$P<0.05$; **$P<0.01$; *** $P<0.001$

to induce cell death, we used a biotinylated 3′G-ODNs to perform protein pull-down assays from rat embryonic brain homogenate. The biotinylated 3′G-ODNs was coupled with streptavidin-coated magnetic beads and then incubated with rat embryonic brain homogenate. To confirm the specificity of protein binding to 3′G-ODNs, the pull-down assay was done in the presence of biotinylated 5′G-ODNs (Fig. 3a). The bound proteins were separated by SDS-PAGE and visualized by Coomassie blue staining (indicated by arrows). To identify the proteins bound to 3′G-ODNs, these proteins were digested by trypsin and analyzed by liquid chromatography mass spectrometry (LC-MS/MS). The protein candidates associated with 3′G-ODNs were identified and are listed in Table 2. Among these candidates, YB-1 had the highest score and sequence coverage (Table 2).

To further verify the association between YB-1 and 3′G-ODNs in embryonic neuron cells, we first pulled down the proteins associated with 3′G-ODNs followed by western blotting using specific antibodies against YB-1, hnRNP H1 and EF1A1. As shown in Fig. 3b, YB-1 formed complexes only with the biotinylated 3′G-ODNs and not with the biotinylated 5′G-ODNs. Rat embryonic brain lysate was used as a control to monitor the evenness of sample input (Fig. 3b). We also performed immunofluorescence staining by using an antibody against YB-1 protein followed by FAM-labeled 3′G-ODNs stimulation and verified that 3′G-ODNs indeed associated with YB-1 in embryonic neuron cells (Fig. 3c). Collectively, these results indicate that 3′G-ODNs associates with YB-1 protein in the cytoplasm after diffusion into embryonic neuron cells.

YB-1 is a key regulator of transcription in adult brain [21] and it has been shown that HSP60 interacts with YB-1 to regulate the subcellular distribution of YB-1 [22]. To elucidate whether 3′G-ODNs association with YB-1 also regulates the cellular localization of YB-1, nuclear and cytoplasmic levels of YB-1 were examined after separation of nuclear and cytoplasmic fractions from embryonic neuron cells. We found that YB-1 protein was predominantly expressed in the cytoplasm of rat embryonic neuron cells and

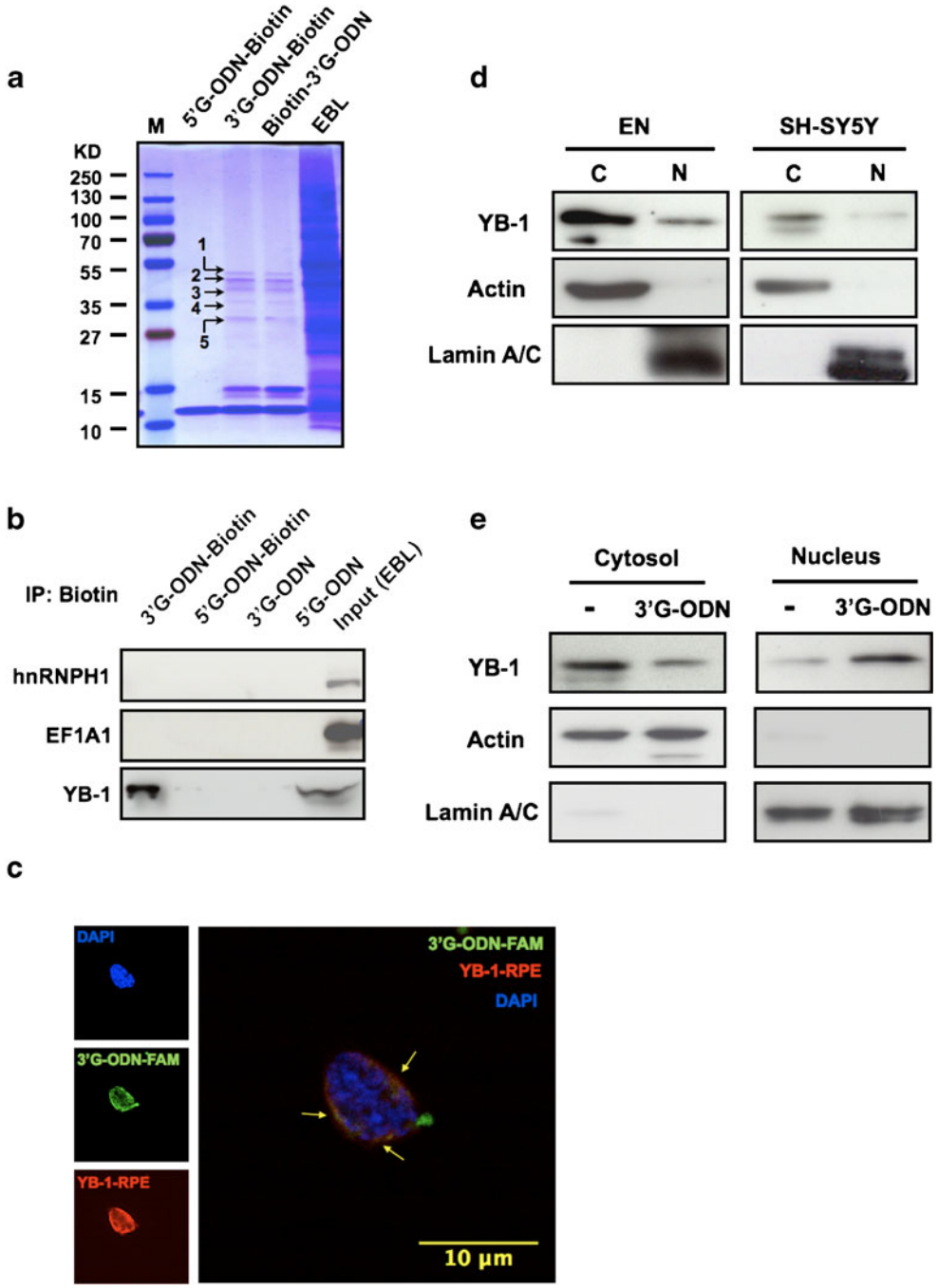

Fig. 3 3′G-ODNs binds Y-box-binding protein (*YB-1*) and increases its translocation into nucleus of embryonic neuron cells. **a** Identification of YB-1 bound to 3′G-ODN by mass spectrometry. Pull-down assays followed by SDS-PAGE were used to isolate 3′G-ODN-bound YB1. Biotinylated 3′G-ODN was incubated with brain lysates from rat embryo, whereupon YB-1 were separated and detected by SDS-PAGE followed by Coomassie staining; excised bands were then subjected to LC-MS/MS analysis. Biotinylated 5′G-ODN was used as negative control and embryonic brain lysate (*EBL*) was the input control. **b** The binding between 3′G-ODN and YB-1 in rat embryonic brain lysates was confirmed by immunoprecipitation (*IP*). Rat brain lysates were incubated with 3′G-ODN-biotin or other control ODNs and immunoprecipitated by using streptavidin-conjugated magnetic beads. The presence of YB-1 in the immunoprecipitates was determined by western blotting with anti-YB-1 antibodies. **c** Colocalization of 3′G-ODN and YB-1 in the cytosol near the nucleus. Prior to immunofluorescence microscopy, embryonic neurons were fixed in 4 % paraformaldehyde and 4 % sucrose after treatment with 6-carboxy-fluo-rescine (*FAM*)-labeled 3′G- ODNs (*3′G-ODN-FAM*) for 2 h. Embryonic neurons were co-stained with anti-YB-1 antibody followed by secondary R-phycoerythrin (*RPE*) conjugated anti-rabbit antibodies. DAPI staining of the nucleus is shown in blue. *Yellow arrows* indicate the interaction between 3′G-ODNs and YB-1. **d** Different localization of YB-1 in the cytoplasm and nucleus of primary embryonic neuron (*EN*) cells or SH-SY5Y human neuroblastoma cell line. **e** YB-1 protein translocated from cytoplasm to nucleus of primary embryonic neuron cells after stimulation with 3′G-ODNs. Lamin A/C and actin were used as loading controls, and fractions of the nuclear and cytosolic extracts from the same protein lysates were assessed

Table 2 Proteins binding to 3′G-ODN identified by LC-MS/MS

Accession no.	Protein	Score(s)	Sequence coverage (%)	Peptide matched no.	MW (kDa)
P62630	Elongation factor 1-alpha 1	114	12	7	50.1
Q8VHV7	Heterogeneous nuclear ribonucleoprotein H	62	8	3	49.2
P68370	Tubulin alpha-1A chain	91	25	9	50.1
P69897	Tubulin beta-5 chain	63	17	6	49.6
P60711	Actin and cytoplasmic 1	53	4	1	41.7
P62961	Nuclease-sensitive element-binding protein 1	325	31	6	35.7
P21533	60S ribosomal protein in L6	70	15	6	33.5
A7VJC2	Heterogeneous nuclear ribonucleoprotein A2/B1	52	7	2	37.5
P04797	Glyceraldehyde-3-phosphate dehydrogenase	36	12	3	35.8
P62997	Transformer-2 protein homolog beta	36	16	4	33.6
P04256	Heterogeneous nuclear ribonucleoprotein A1	30	5	1	34.2

SH-SY5Y human neuroblastoma cells (Fig. 3d). As shown in Fig. 3e, the level of nuclear YB-1 was increased after stimulation with 3′G-ODNs, whereas the level of cytoplasmic YB-1 was decreased in embryonic neuron cells (Fig. 3e). These results indicate that nuclear translocation of YB-1 is enhanced in embryonic neuron cells after binding to 3′G-ODNs.

An YB-1 Mutant Lacking the Nuclear Localizing Sequence Results in Insensitivity of Embryonic Neuron Cells to Cytotoxicity Induced by 3′G-ODNs

To examine whether YB-1 translocation is important for cell cytotoxicity induced by 3′G-ODNs, we constructed an YB-1-dNLS (deletion of nuclear localization sequence) plasmid that is without nuclear localization sequence. We found wild-type YB-1 protein was located in the cytoplasm and nucleus of neuro-2a cells, whereas the expression of YB-1-dNLS mutant protein was found to locate only in the cytoplasm of neuro-2a cells (Fig. 4a). The 3′G-ODNs-mediated neuronal cytotoxicity was attenuated in embryonic neuron cells overexpressing YB-1-dNLS mutant protein as compared with YB-1-overexpressing embryonic neuron cells (Fig. 4b). The number of PI-positive cells and caspase 3/7 activities in neurons overexpressing YB-1-dNLS mutant was lower than that in cells overexpressing YB-1 after 3′G-ODNs treatment (Fig. 4c, d). Together, these results indicate that embryonic neuron cells overexpressing YB-1-dNLS mutant protein block the cytotoxic effect induced by 3′G-ODNs and suggest that translocation of YB-1 to the nucleus is important for the cytotoxic effect of 3′G-ODNs.

F-spondin Expression Is Repressed by 3′G-ODNs in Embryonic Neuron Cells

F-spondin mediates the survival pathway in murine neuroblastoma [16] and chicken ciliary ganglion [17]. To determine whether F-spondin expression was affected by 3′G-ODNs, we first examined F-spondin protein expression in embryonic neuron cells. We found that F-spondin was expressed in embryonic neuron cells and was predominantly expressed in PC-12, neuro-2a, and SH-SY5H neuroblastoma cells (Fig. 4 in the ESM). Next, total RNA was extracted from embryonic neuron cells treated with 3′G-ODNs, and then the transcriptional level of F-spondin was examined by real-time PCR. F-spondin RNA expression levels in embryonic neuron cells stimulated with 3′G-ODNs were lower than those without any stimulation (Fig. 5a). The protein expression of F-spondin was also markedly decreased in 3′G-ODNs-treated embryonic neuron cells (Fig. 5b). In order to ascertain that 3′G-ODNs decreased F-spondin expression through YB-1 translocation to the nucleus, we detected F-spondin protein expression in embryonic neuron cells transfected with YB-1 or YB-1-dNLS mutant plasmid after 3′G-ODNs stimulation. We first confirmed the success of transfection by fluorescence microscopy (Fig. 5 in the ESM) and then treated the cells with 3′G-ODNs. We found that 3′G-ODNs treatment for 24 h decreased F-spondin protein expression in embryonic neuron cells transfected with YB-1 plasmid, but not in embryonic neuron cells overexpressing YB-1-dNLS (Fig. 5c). Taken together, these findings suggest that 3′G-ODNs downregulates F-spondin expression in embryonic neuron cells at both transcriptional and translational levels through YB-1 translocation into the nucleus.

YB-1 Translocates to the Nucleus and Binds to the Promoter of F-spondin

YB-1 is involved in a variety of cellular functions. It regulates DNA transcription, RNA processing and translational control of protein synthesis [23, 24]. An inverted CCAAT-box found in the HLA class II gene promoter was originally determined as YB-1-binding motif [25]. We examined whether the promoter of F-spondin contains an YB-1-

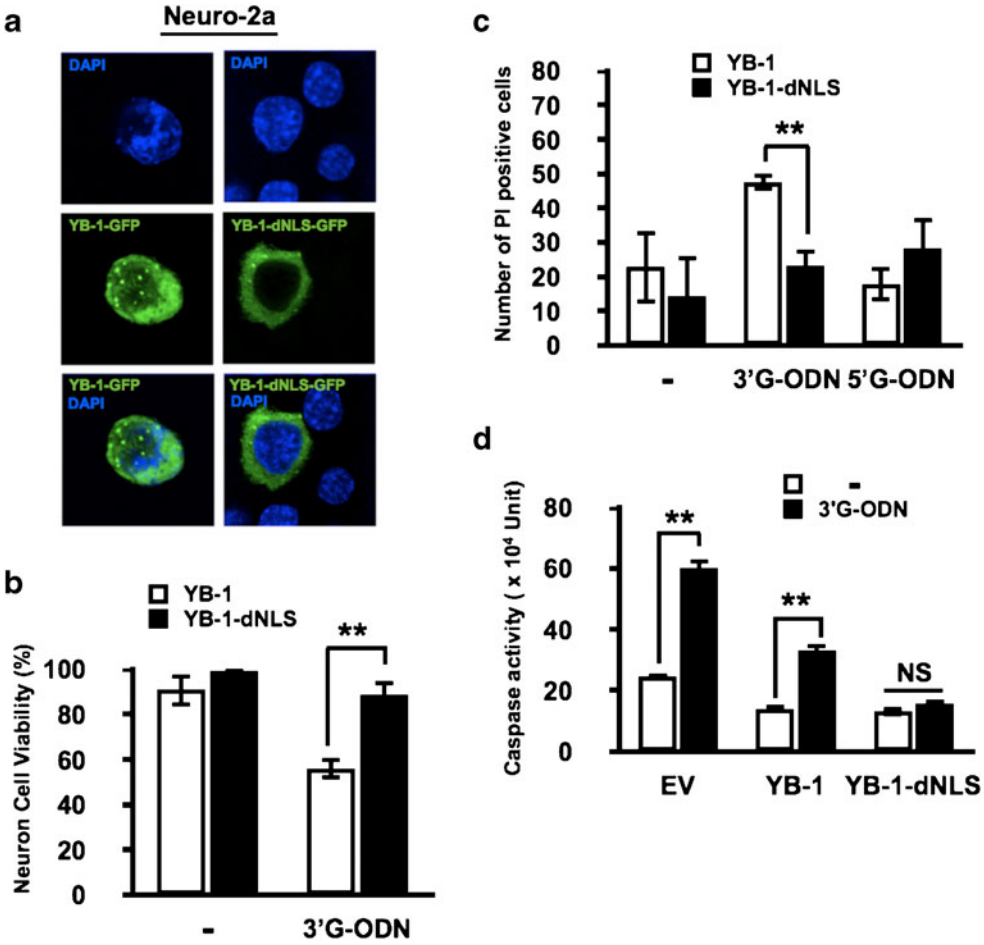

Fig. 4 YB-1 deletion NLS mutant (*YB-1-dNLS*) attenuates 3′G-ODNs-mediated cytotoxicity and caspase activity in embryonic neuron cells. **a** Subcellular localization of YB-1 and YB-1-dNLS in neuro-2a cells. Neuro-2a cells were transfected with either YB-1 or YB-1-dNLS plasmid construct. Localization of YB-1 in neuro-2a cells was detected by GFP fluorescence. The nuclei of cells were labeled with DAPI (*blue*). **b** Embryonic neuron cells were transfected with YB-1 or YB-1-dNLS plasmid for 48 h, and cultured for another 48 h in neurobasal medium in the presence of 2 μM 3′G-ODN. MTS assay was used to determine cell viability. **c** Percentage of damaged embryonic neuron cells was detected by using propidium iodide (*PI*) staining after 48-h incubation with 2 μM 5′G-ODN or 3′G-ODN. **d** The caspase 3/7 activities in the lysates of empty vector (*EV*), YB-1, and YB-1-dNLS-transfected embryonic neuron cells were estimated after stimulation with or without 2 μM 3′G-ODN for 48 h as indicated. Data represent the mean±SD; $N=3$; $^{**}P<0.01$; *NS* not significant

binding motif (inverted CCAAT-box) using the Transcription Element Search System website. We found several YB-1-binding motifs within the promoter of F-spondin (Fig. 5d). We also confirmed that YB-1 binds to the promoter region of F-spondin at the −45 and −1,137 ATTGG sites by ChIP assay (Fig. 5e). These results indicate that YB-1 interacts with the promoter of F-spondin and serves as a repressor of F-spondin transcription in embryonic neuron cells.

Ectopic Expression of F-spondin Protein Renders Embryonic Neuron Cells More Resistant to 3′G-ODNs-Mediated Cell Death

Since 3′G-ODNs induces neuron cell death through enhancement of YB-1 translocation to the nucleus, which then represses F-spondin transcription, we further examined whether overexpression of F-spondin in embryonic neuron cells could reverse the effect induced by 3′G-ODNs. GFP-fused F-spondin protein was overexpressed in embryonic neuron cells in order to trace and calculate neurite length by Image J software. F-spondin protein was detected in embryonic neuron cells transfected with mock or spon1-GFP plasmid by western blotting (Fig. 6a). Treatment with 3′G-ODNs for 16 h decreased the mean neurite length of mock-transfected embryonic neuron cells but not that of F-spondin overexpressing embryonic neuron cells (Fig. 6b). To further confirm that 3′G-ODNs induced neuron cell death through F-spondin elimination, embryonic neuron cells were transiently transfected with mock or biotin-spon1 plasmid, and then stimulated with 3′G-ODNs for 48 h. Our results showed that ectopic expression of F-spondin led to overexpression of biotin-fused F-spondin (Fig. 6c) and tolerance to 3′G-ODNs-mediated cell cytotoxicity in embryonic neuron cells as compared with the mock-transfected group (Fig. 6d). The caspase 3/7 activities in embryonic neurons overexpressing F-spondin were also lower than those in the mock group after 3′G-ODNs treatment (Fig. 6e). Taken together, these results suggest that F-spondin protects embryonic neuron cells against cytotoxic effects induced by 3′G-ODNs.

Discussion

G-rich oligodeoxynucleotides (G-ODNs) have been shown to exhibit antiproliferative activity and to induce apoptosis

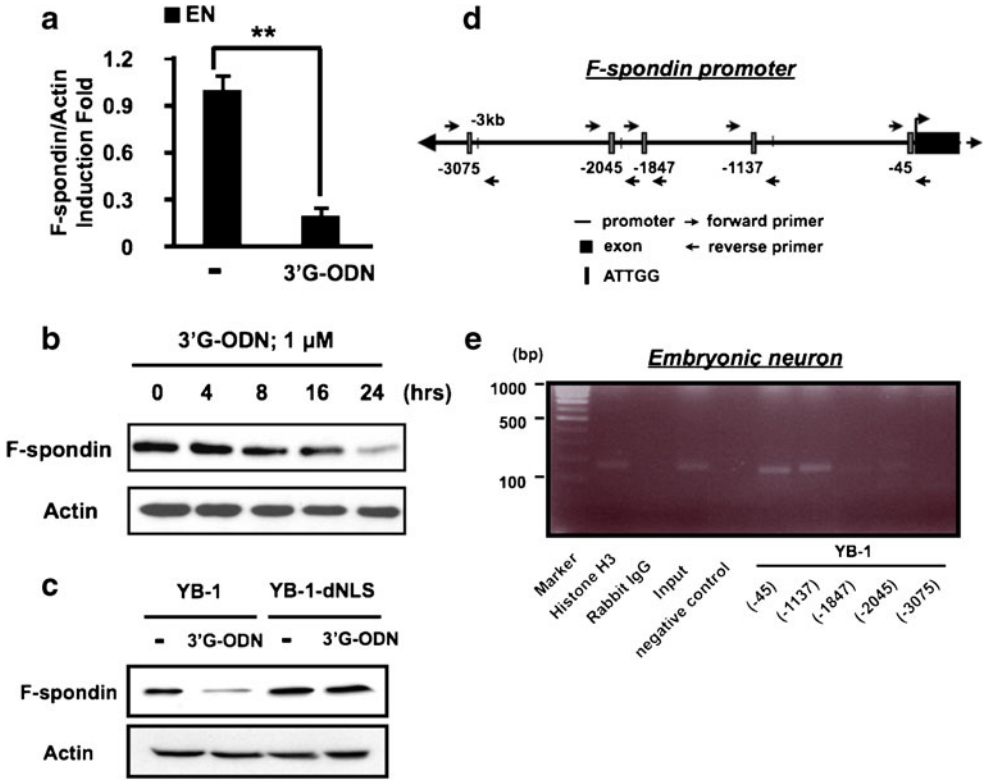

Fig. 5 3′G-ODNs decreases F-spondin expression in embryonic neuron cells by promoting the translocation of YB-1 into nucleus to suppress F-spondin promoter. **a** Treatment with 3′G-ODNs decreased F-spondin expression in embryonic neuron cells. Total RNA was prepared to examine F-spondin expression by quantitative Real-Time PCR analysis. β-actin was used as a loading control. The induction folds of F-spondin in 3′G-ODN-treated and untreated cells were plotted. Data represent the mean±SD; $^{**}P<0.01$. **b** Cell lysates of embryonic neuron cells treated with 3′G-ODN for the indicated times were prepared. F-spondin protein level was analyzed by western blotting. Actin was used as a loading control. **c** Western blotting analysis of F-spondin protein expression in YB-1 overexpressing and YB-1-dNLS expressing embryonic neuron cells in response to 3′G-ODN treatment. **d** Schematic drawing of the potential YB-1-binding sites on F-spondin promoter. Primers were designed to amply the ATTGG sites within the promoter of F-spondin. **e** Embryonic neuron cells were subjected to chromatin immunoprecipitation, and the DNA complexes isolated were amplified with F-spondin primers to confirm endogeneous YB-1 binding. There was no nonspecific binding to the IgG control (*lane 2*), and the input DNA served as a positive control (*lane 3*). Binding between YB-1 and F-spondin promoter was observed in *lanes 5* and *6*

in tumor cell lines [26–29]. Although there are a number of reports describing the apoptosis-inducing ability of these G-ODNs, the motif or sequence responsible for inducing cytotoxicity are still unclear. In this study, we clearly demonstrated that G-ODNs also have the ability to induce cytotoxicity and neurite retraction in neuron cells besides cancer cells. We also defined further the 3′G but not 5′G motif being responsible for inducing cytotoxicity and identifed YB-1 protein as most likely target of 3′G-ODNs, thereby unraveling the mechanisms involved in the eventual cytotoxicity of 3′G-ODNs in embryonic neuron cells.

We determined that a poly-G at the 3′ terminus was sufficient to generate cytotoxic activity of G-ODNs in embryonic neuron cells; by contrast, a cytotoxic effect was not elicited if poly-G was present at the 5′ terminus. This finding thus indicates that the cytotoxic effect of G-ODNs requires a 3′poly-G motif. In order to examine whether the 3′G-ODNs used in this study self-assemble to form higher-order structure, we performed gel electrophoresis with ODN2216 that has been demonstrated to exhibit tertiary structures [7] and 3′G-ODN. Under non-denaturing conditions, a small portion of 3′G-ODN appeared at a higher molecular weight position (Fig. 6 in the ESM), indicating spontaneous multi-merization of 3′G-ODNs. It is likely that the higher-order structure formed through multi-merization of 3′G-ODNs is important for its effect in embryonic neuron cells. Nevertheless, whether this higher-order structure represents quadruplex structure awaits further investigation.

A previous study reported that G-ODNs reduce cell growth in human carcinoma via downregulation of the expression of the Ki-*ras* oncogene [27]. However, we found a totally different mechanism by which G-ODNs induces cytotoxicity in embryonic neuron cells. Using a pull-down analysis, we showed that the transcription factor YB-1 interacted with 3′G-ODN in the cytoplasm of embryonic neuron cells (Fig. 3). YB-1 has been reported to interact with the

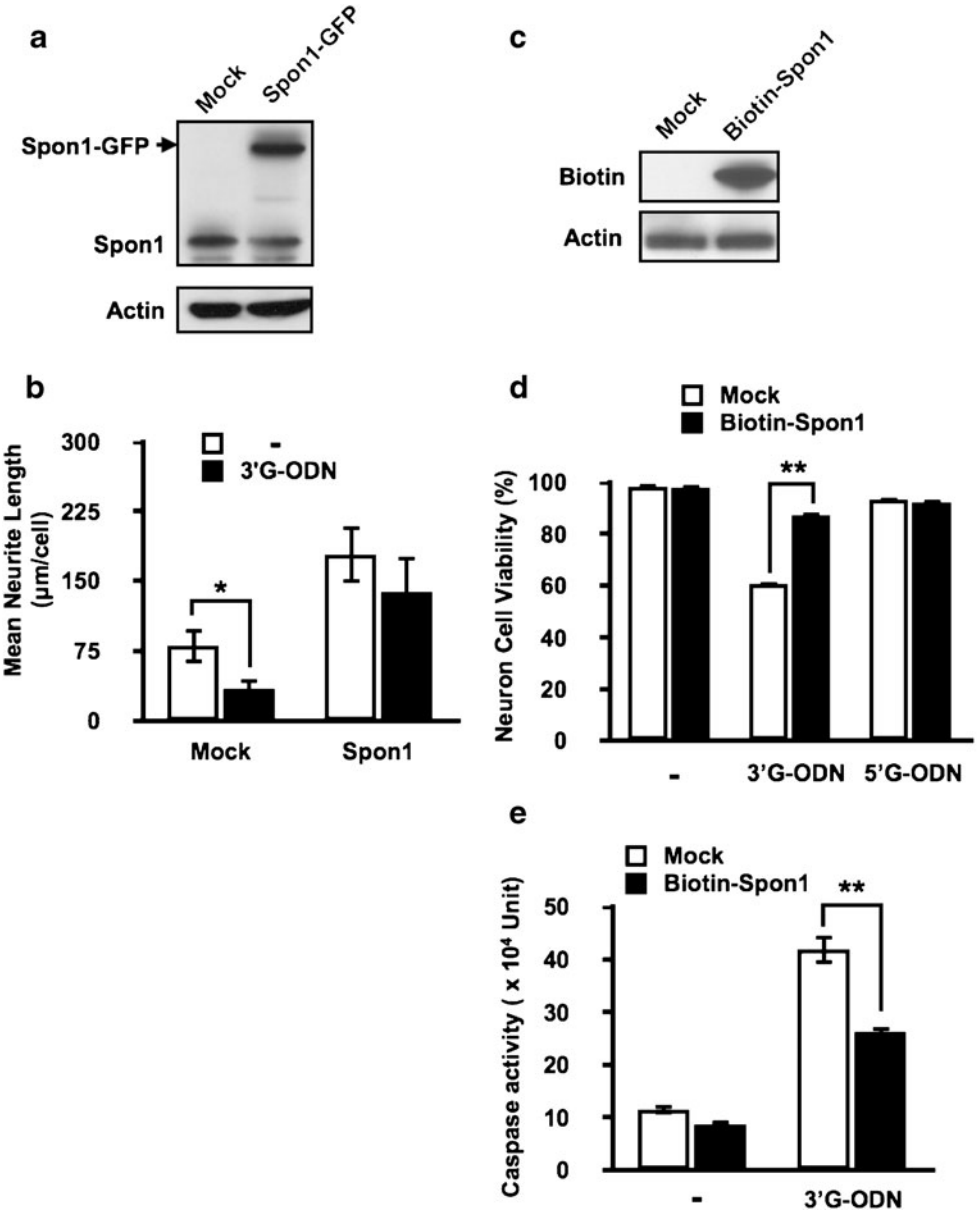

Fig. 6 Over-expression of F-spondin provides protection against 3′G-ODN-induced neurite contraction and cytotoxicity in embryonic neuron cells. **a** Over-expression of GFP fused F-spondin protein in embryonic neuron cells. F-spondin was detected with anti-F-spondin antibodies by western blotting. Actin was used as loading controls. **b** Forty-eight hours after transfection with mock or spon1-GFP plasmid, embryonic neuron cells were treated with 1 μM 3′G-ODN at 37 °C for 16 h. Neurite length of untreated and 3′G-ODN-treated cells was quantified by tracing GFP with Image J software. **c** Embryonic neuron cells were transfected with mock or biotin-fused F-spondin plasmid, and the success of transfection was confirmed by western blotting analysis with anti-biotin antibodies. **d** Embryonic neuron cells that had been transfected with mock or biotin fused F-spondin plasmid were cultured for 48 h in the presence of 5′G-ODN or 3′G-ODN. MTS assay was used to determine cell viability. **e** The caspase 3/7 activities in embryonic neuron cells treated as indicated were estimated. Data represent the mean±SD; $N=3$; $^{*}P<0.05$; $^{**}P<0.01$

serotonin transporter gene and may be associated with a number of neurological disorders [30]. Furthermore, in our study, YB-1 protein expression was enhanced in the nucleus by 3′G-ODN treatment, thus repressing F-spondin expression and leading to neurotoxicity (Figs. 3, 4, and 5). F-spondin is an important protein for neuron development [31] and neuron cell survival [16, 17]. Therefore, it will be interesting to further study whether inhibition of F-spondin protein by YB-1 also involves in certain neurological disorders.

YB-1 has been shown to interact with other transcription factors and viral proteins [32–34]. In addition, previous studies suggested that the level of Sp1 activity dictates binding of YB-1 to its target sequence and therefore affects its regulatory function [35, 36]. Thus, it could be argued that YB-1 and Sp1 regulate F-spondin transcription through their physical interactions. However, it remains to be elucidated whether the transcription factor Sp1 also regulates F-spondin expression in embryonic neuron cells. Moreover, YB-1 is known to involve in neural tube closure in early mouse development [37], and it also restores the neurite outgrowth inhibition induced by Sox21 [38]. In our study, however, we found that 3′G-ODN promoted YB-1 translocation into nucleus which then repressed F-spondin expression and further caused cell death and neurite retraction. One possible explanation for this opposite effect of YB-1 may be the temporal and spatial distribution of YB-1 in neuron cells. Although F-spondin has been reported to be associated with neuron development, the exact mechanism is still unclear. After the proteolysis of F-spondin, each part of F-spondin has opposite effect on signal guidance of commissural neuron extension [39]. Therefore, it will be

interesting to further study the detailed mechanism by which YB-1 regulates F-spondin or other neurite outgrowth related protein in embryonic neuron cells.

Patients infected with human immunodeficiency virus (HIV) develop dementia and encephalitis [40], which result from the apoptotic death of infected neurons. However, the precise underlying pathogenetic mechanism of HIV-induced neuronal injury is not fully elucidated. Previously, it has been reported that HIV-1 central DNA flap (+) strand-derived ODNs form an intermolecular parallel DNA quadruplex structure [41]. This G-quadruplex structure has been shown to directly interact with the HIV-1 nucleocapsid protein and further generates a subviral particle termed the pre-integration complex (PIC) [42–44]. Our study has showed that 3′G-ODNs, that are capable of forming higher-order structures like G-quadruplex-forming ODNs, induce embryonic neuron cell death through enhancement of YB-1 translocation to the nucleus and repression of F-spondin expression. It provides the possibility that HIV-1-induced neuron cell injury may occur through inhibition of F-spondin protein expression in neuron cells.

Altogether, our results show that the induction of neurite retraction and cytotoxicity in embryonic neuron cells by 3′G-rich ODNs is due to a reduction in F-spondin expression. Furthermore, we have demonstrated that the transcription factor YB-1 is responsible for the 3′G-rich ODN-elicited repression of F-spondin expression and induction of cytotoxicity in embryonic neuron cells. We plan to examine if similar mechanisms occur in cancer cells, such as neuroblastoma cells in the future. Despite that, the results presented herein suggest that the 3′G-ODNs may cause cytotoxicity in neurons in addition to metastatic cancer cells as demonstrated in other studies. Thus, their potentiality as therapeutic drugs for metastatic cancers requires careful evaluation.

Acknowledgments This study was supported by grants from Academia Sinica (94F006 to SM Liang) and the National Science Council (NSC 93-2317-B-001-003 to SM Liang) of Taiwan.

References

1. Tokunaga T, Yamamoto H, Shimada S, Abe H, Fukuda T, Fujisawa Y, Furutani Y, Yano O, Kataoka T, Sudo T et al (1984) Antitumor activity of deoxyribonucleic acid fraction from *Mycobacterium bovis* BCG. I. Isolation, physicochemical characterization, and antitumor activity. J Natl Cancer Inst 72(4):955–962
2. Krieg AM, Yi AK, Matson S, Waldschmidt TJ, Bishop GA, Teasdale R, Koretzky GA, Klinman DM (1995) CpG motifs in bacterial DNA trigger direct B-cell activation. Nature 374 (6522):546–549. doi:10.1038/374546a0
3. Yamamoto S, Yamamoto T, Kataoka T, Kuramoto E, Yano O, Tokunaga T (1992) Unique palindromic sequences in synthetic oligonucleotides are required to induce IFN [correction of INF] and augment IFN-mediated [correction of INF] natural killer activity. J Immunol 148(12):4072–4076
4. Hartmann G, Weiner GJ, Krieg AM (1999) CpG DNA: a potent signal for growth, activation, and maturation of human dendritic cells. Proc Natl Acad Sci USA 96(16):9305–9310
5. Lenert P, Rasmussen W, Ashman RF, Ballas ZK (2003) Structural characterization of the inhibitory DNA motif for the type A (D)-CpG-induced cytokine secretion and NK-cell lytic activity in mouse spleen cells. DNA Cell Biol 22(10):621–631. doi:10.1089/104454903770238094
6. Verthelyi D, Zeuner RA (2003) Differential signaling by CpG DNA in DCs and B cells: not just TLR9. Trends Immunol 24(10):519–522
7. Kerkmann M, Costa LT, Richter C, Rothenfusser S, Battiany J, Hornung V, Johnson J, Englert S, Ketterer T, Heckl W, Thalhammer S, Endres S, Hartmann G (2005) Spontaneous formation of nucleic acid-based nanoparticles is responsible for high interferon-alpha induction by CpG-A in plasmacytoid dendritic cells. J Biol Chem 280(9):8086–8093. doi:10.1074/jbc.M410868200
8. Gilbert DE, Feigon J (1999) Multistranded DNA structures. Curr Opin Struct Biol 9(3):305–314. doi:10.1016/S0959-440X(99)80041-4
9. Williamson JR (1994) G-quartet structures in telomeric DNA. Annu Rev Biophys Biomol Struct 23:703–730. doi:10.1146/annurev.bb.23.060194.003415
10. Jing N, Li Y, Xu X, Sha W, Li P, Feng L, Tweardy DJ (2003) Targeting Stat3 with G-quartet oligodeoxynucleotides in human cancer cells. DNA Cell Biol 22(11):685–696. doi:10.1089/104454903770946665
11. Burstyn-Cohen T, Frumkin A, Xu YT, Scherer SS, Klar A (1998) Accumulation of F-spondin in injured peripheral nerve promotes the outgrowth of sensory axons. J Neurosci 18(21):8875–8885
12. Higashijima S, Nose A, Eguchi G, Hotta Y, Okamoto H (1997) Mindin/F-spondin family: novel ECM proteins expressed in the zebrafish embryonic axis. Dev Biol 192(2):211–227
13. Ruiz i Altaba A, Cox C, Jessell TM, Klar A (1993) Ectopic neural expression of a floor plate marker in frog embryos injected with the midline transcription factor Pintallavis. Proc Natl Acad Sci USA 90(17):8268–8272
14. Schubert D, Klar A, Park M, Dargusch R, Fischer WH (2006) F-spondin promotes nerve precursor differentiation. J Neurochem 96 (2):444–453. doi:10.1111/j.1471-4159.2005.03563.x
15. Nagarajan G, Kuo CC, Liang CM, Chen CM, Liang SM (2007) Effects of CpG-B ODN on the protein expression profile of swine PBMC. Vet Res 38(6):795–808. doi:10.1051/vetres:2007032
16. Cheng YC, Liang CM, Chen YP, Tsai IH, Kuo CC, Liang SM (2009) F-spondin plays a critical role in murine neuroblastoma survival by maintaining IL-6 expression. J Neurochem 110 (3):947–955. doi:10.1111/j.1471-4159.2009.06186.x
17. Peterziel H, Sackmann T, Strelau J, Kuhn PH, Lichtenthaler SF, Marom K, Klar A, Unsicker K (2011) F-spondin regulates neuronal survival through activation of disabled-1 in the chicken ciliary ganglion. Mol Cell Neurosci 46(2):483–497. doi:10.1016/j.mcn.2010.12.001
18. Brewer GJ, Torricelli JR (2007) Isolation and culture of adult neurons and neurospheres. Nat Protoc 2(6):1490–1498. doi:10.1038/nprot.2007.207
19. Chung CW, Hong YM, Song S, Woo HN, Choi YH, Rohn T, Jung YK (2003) Atypical role of proximal caspase-8 in truncated Tau-induced neurite regression and neuronal cell death. Neurobiol Dis 14(3):557–566
20. Ye C, Zhang Y, Wang W, Wang J, Li H (2008) Inhibition of neurite outgrowth and promotion of cell death by cytoplasmic soluble mutant huntingtin stably transfected in mouse neuroblastoma cells. Neurosci Lett 442(1):63–68. doi:10.1016/j.neulet.2008.05.119
21. Unkruer B, Pekcec A, Fuest C, Wehmeyer A, Balda MS, Horn A, Baumgartner W, Potschka H (2009) Cellular localization of Y-box binding protein 1 in brain tissue of rats, macaques, and humans. BMC Neurosci 10:28. doi:10.1186/1471-2202-10-28

22. Ohashi S, Atsumi M, Kobayashi S (2009) HSP60 interacts with YB-1 and affects its polysome association and subcellular localization. Biochem Biophys Res Commun 385(4):545–550. doi:10.1016/j.bbrc.2009.05.094
23. Evdokimova V, Ovchinnikov LP, Sorensen PH (2006) Y-box binding protein 1: providing a new angle on translational regulation. Cell Cycle 5(11):1143–1147
24. Matsumoto K, Wolffe AP (1998) Gene regulation by Y-box proteins: coupling control of transcription and translation. Trends Cell Biol 8(8):318–323
25. Didier DK, Schiffenbauer J, Woulfe SL, Zacheis M, Schwartz BD (1988) Characterization of the cDNA encoding a protein binding to the major histocompatibility complex class II Y box. Proc Natl Acad Sci USA 85(19):7322–7326
26. Choi EW, Nayak LV, Bates PJ (2010) Cancer-selective antiproliferative activity is a general property of some G-rich oligodeoxynucleotides. Nucleic Acids Res 38(5):1623–1635. doi:10.1093/nar/gkp1088
27. Cogoi S, Quadrifoglio F, Xodo LE (2004) G-rich oligonucleotide inhibits the binding of a nuclear protein to the Ki-ras promoter and strongly reduces cell growth in human carcinoma pancreatic cells. Biochemistry 43(9):2512–2523. doi:10.1021/bi035754f
28. Qi H, Lin CP, Fu X, Wood LM, Liu AA, Tsai YC, Chen Y, Barbieri CM, Pilch DS, Liu LF (2006) G-quadruplexes induce apoptosis in tumor cells. Cancer Res 66(24):11808–11816. doi:10.1158/0008-5472.CAN-06-1225
29. Schwartz TR, Vasta CA, Bauer TL, Parekh-Olmedo H, Kmiec EB (2008) G-rich oligonucleotides alter cell cycle progression and induce apoptosis specifically in OE19 esophageal tumor cells. Oligonucleotides 18(1):51–63. doi:10.1089/oli.2007.0109
30. Klenova E, Scott AC, Roberts J, Shamsuddin S, Lovejoy EA, Bergmann S, Bubb VJ, Royer HD, Quinn JP (2004) YB-1 and CTCF differentially regulate the 5-HTT polymorphic intron 2 enhancer which predisposes to a variety of neurological disorders. J Neurosci 24(26):5966–5973. doi:10.1523/JNEUROSCI.1150-04.200424/26/5966
31. Benard C, Hobert O (2009) Looking beyond development: maintaining nervous system architecture. Curr Top Dev Biol 87:175–194. doi:10.1016/S0070-2153(09)01206-X
32. Chernukhin IV, Shamsuddin S, Robinson AF, Carne AF, Paul A, El-Kady AI, Lobanenkov VV, Klenova EM (2000) Physical and functional interaction between two pluripotent proteins, the Y-box DNA/RNA-binding factor, YB-1, and the multivalent zinc finger factor, CTCF. J Biol Chem 275(38):29915–29921. doi:10.1074/jbc.M001538200
33. Okamoto T, Izumi H, Imamura T, Takano H, Ise T, Uchiumi T, Kuwano M, Kohno K (2000) Direct interaction of p53 with the Y-box binding protein, YB-1: a mechanism for regulation of human gene expression. Oncogene 19(54):6194–6202. doi:10.1038/sj.onc.1204029
34. Safak M, Gallia GL, Ansari SA, Khalili K (1999) Physical and functional interaction between the Y-box binding protein YB-1 and human polyomavirus JC virus large T antigen. J Virol 73 (12):10146–10157
35. Higashi K, Inagaki Y, Suzuki N, Mitsui S, Mauviel A, Kaneko H, Nakatsuka I (2003) Y-box-binding protein YB-1 mediates transcriptional repression of human alpha 2(I) collagen gene expression by interferon-gamma. J Biol Chem 278(7):5156–5162. doi:10.1074/jbc.M208724200
36. Sawaya BE, Khalili K, Amini S (1998) Transcription of the human immunodeficiency virus type 1 (HIV-1) promoter in central nervous system cells: effect of YB-1 on expression of the HIV-1 long terminal repeat. J Gen Virol 79(Pt 2):239–246
37. Uchiumi T, Fotovati A, Sasaguri T, Shibahara K, Shimada T, Fukuda T, Nakamura T, Izumi H, Tsuzuki T, Kuwano M, Kohno K (2006) YB-1 is important for an early stage embryonic development: neural tube formation and cell proliferation. J Biol Chem 281(52):40440–40449. doi:10.1074/jbc.M605948200
38. Ohba H, Chiyoda T, Endo E, Yano M, Hayakawa Y, Sakaguchi M, Darnell RB, Okano HJ, Okano H (2004) Sox21 is a repressor of neuronal differentiation and is antagonized by YB-1. Neurosci Lett 358(3):157–160. doi:10.1016/j.neulet.2004.01.026
39. Zisman S, Marom K, Avraham O, Rinsky-Halivni L, Gai U, Kligun G, Tzarfaty-Majar V, Suzuki T, Klar A (2007) Proteolysis and membrane capture of F-spondin generates combinatorial guidance cues from a single molecule. J Cell Biol 178(7):1237–1249. doi:10.1083/jcb.200702184
40. Gonzalez-Scarano F, Martin-Garcia J (2005) The neuropathogenesis of AIDS. Nat Rev Immunol 5(1):69–81. doi:10.1038/nri1527
41. Lyonnais S, Hounsou C, Teulade-Fichou MP, Jeusset J, Le Cam E, Mirambeau G (2002) G-quartets assembly within a G-rich DNA flap. A possible event at the center of the HIV-1 genome. Nucleic Acids Res 30(23):5276–5283
42. Bukrinsky MI, Sharova N, McDonald TL, Pushkarskaya T, Tarpley WG, Stevenson M (1993) Association of integrase, matrix, and reverse transcriptase antigens of human immunodeficiency virus type 1 with viral nucleic acids following acute infection. Proc Natl Acad Sci USA 90(13):6125–6129
43. Fassati A, Goff SP (2001) Characterization of intracellular reverse transcription complexes of human immunodeficiency virus type 1. J Virol 75(8):3626–3635. doi:10.1128/JVI.75.8.3626-3635.2001
44. Miller MD, Farnet CM, Bushman FD (1997) Human immunodeficiency virus type 1 preintegration complexes: studies of organization and composition. J Virol 71(7):5382–5390